Functional Effects of Auxiliary β4-Subunit on Rat Large-Conductance Ca^{2+}-Activated K^+ Channel

Tal Soo Ha, Moon-Sun Heo, and Chul-Seung Park
Laboratory of Molecular Neurobiology, Department of Life Science, Kwangju Institute of Science and Technology, Gwangju, 500-712, Korea

ABSTRACT Large-conductance calcium-activated potassium (BK_{Ca}) channels are composed of the pore-forming α-subunit and the auxiliary β-subunits. The β4-subunit is dominantly expressed in the mammalian central nervous system. To understand the physiological roles of the β4-subunit on the BK_{Ca} channel α-subunit (Slo), we isolated a full-length complementary DNA of rat β4-subunit (rβ4), expressed heterolgously in *Xenopus* oocytes, and investigated the detailed functional effects using electrophysiological means. When expressed together with rat Slo (rSlo), rβ4 profoundly altered the gating characteristics of the Slo channel. At a given concentration of intracellular Ca^{2+}, rSlo/rβ4 channels were more sensitive to transmembrane voltage changes. The activation and deactivation rates of macroscopic currents were decreased in a Ca^{2+}-dependent manner. The channel activation by Ca^{2+} became more cooperative by the coexpression of rβ4. Single-channel recordings showed that the increased Hill coefficient for Ca^{2+} was due to the changes in the open probability of the rSlo/rβ4 channel. Single BK_{Ca} channels composed of rSlo and rβ4 also exhibited slower kinetics for steady-state gating compared with rSlo channels. Dwell times of both open and closed events were significantly increased. Because BK_{Ca} channels are known to modulate neuroexcitability and the expression of the β4-subunit is highly concentrated in certain subregions of brain, the electrophysiological properties of individual neurons should be affected profoundly by the expression of this second subunit.

INTRODUCTION

The large-conductance calcium-activated potassium channels (BK_{Ca} or Maxi-K channels) are a family of potassium-selective ion channels activated in response to the increased intracellular calcium concentration and the transmembrane voltages (for review, Sah, 1996; Toro et al., 1998; Weiger et al., 2002). BK_{Ca} channels are found in a variety of both electrically excitable and nonexcitable cells (Jan and Jan, 1997). Their activities play a key role in neuronal signaling, because they are involved in regulation of transmitter release and repolarization of action potentials (Robitaille and Charlton, 1992; Robitaille et al., 1993; Bielefeldt and Jackson, 1994; Kaczorowski et al., 1996). A single gene, *slowpoke* (*slo*), was initially identified to encode BK_{Ca} channels in *Drosophila* and the molecular cloning of mammalian ortholog (*Slo*) were soon followed (Atkinson et al., 1991; Adelman et al., 1992; Butler et al., 1993; Tseng-Crank et al., 1994; Rosenblatt et al., 1997; Ha et al., 2000). The Slo protein alone can form functional potassium channels of Ca^{2+} and voltage dependence, and a wide range of functionally different BK_{Ca} channels can be expressed by the extensive splicing variations of Slo RNA as well as the modulation of channel activity through intracellular signaling mechanism (Shipston, 2001; Tian et al., 2001). In addition to the Slo protein (α-subunit), the second subunits (β-subunits) of BK_{Ca} channels were identified in higher mammals. The coexpression of the auxiliary β-subunits can change the biophysical and pharmacological properties of the channel composed of only α-subunits (McManus et al., 1995; Valverde et al., 1999; Wallner et al., 1999; Xia et al., 1999; Qian et al., 2002).

Four distinct β-subunits of the BK_{Ca} channel were identified and their genes were cloned from various sources. Although the coexpression of the β1-subunit with the BK_{Ca} α-subunit was found to increase Ca^{2+} sensitivity, slow gating kinetics, and alter pharmacological properties (McManus et al., 1995; Knaus et al., 1994; Dworetzky et al., 1996), the β2-subunit resulted in rapid and complete inactivation of BK_{Ca} currents (Wallner et al., 1999; Xia et al., 1999; Uebele et al., 2000). The β3-subunit also inactivated the BK_{Ca} channel currents rapidly but incompletely. This subunit increased the rate of current activation at moderate Ca^{2+} concentration and induced inward rectification of the current-voltage relationship (Uebele et al., 2000; Brenner et al., 2000; Xia et al., 2000). The β4-subunit was most recently identified and its complementary DNAs (cDNAs) were cloned from human and mouse. The β4-subunit of BK_{Ca} channels was shown to express exclusively in neuronal tissues including cerebral cortex, cerebellum, hippocampus, pons, medulla, thalamus, spinal cord, and so on. Although the β4-subunit is dominantly expressed in brain, the coexpression of this subunit affects the properties of macroscopic BK_{Ca} channel currents only in a modest manner (Brenner et al., 2000; Behrens et al., 2000; Weiger et al., 2000). It was noticed that the coexpression of human β4-subunit slowed down the activation and the deactivation rate of human Slo expressed in heterologous systems. Although the β4-subunit certainly affected the Ca^{2+}-dependent activation of macroscopic human Slo currents, the effect of the β4-subunit was

Submitted December 3, 2003, and accepted for publication January 12, 2004.

Address reprint requests to Chul-Seung Park, PhD, Laboratory of Molecular Neurobiology, Dept. of Life Science, Kwangju Institute of Science and Technology, 1 Oryong-dong, Buk-gu, Gwangju, 500-712, Korea. Tel.: 82-62-970-2489; Fax: 82-62-970-2484; E-mail: cspark@kjist.ac.kr.

0006-3495/04/05/2871/12 $2.00

somewhat inconsistent among the previous reports (Brenner et al., 2000; Behrens et al., 2000; Weiger et al., 2000). Thus, to understand its physiological roles in neuronal cells, it is important to understand the detailed functional effects of the β4-subunit.

In this study, we investigated the electrophysiological effects of rat β4-subunit at the level of both macroscopic and single-channel currents in various concentrations of intracellular Ca^{2+}. We first isolated the full-length cDNA of the β4-subunit from the rat brain library and expressed in *Xenopus* oocytes together with rSlo. This study shows that the β4-subunit increases the sensitivity for voltage and the cooperativity for intracellular Ca^{2+}. The β4-subunit markedly alters the gating behavior of BK_{Ca} channels. The activation and deactivation rates are significantly lowered by the coexpression of the β4-subunit, as shown in a previous study. However, the effects were highly dependent upon the intracellular concentration of Ca^{2+}. In addition, the single-channel recordings revealed that the steady-state gating kinetics rSlo/rβ4 channels were much slower than that of rSlo. Therefore, the β4-subunit affects the electrophysiological activity of the BK_{Ca} channel α-subunit and thus may modulate the excitability of the neuron accordingly.

MATERIALS AND METHODS

Isolation of cDNA for rat BK_{Ca} channel β4-subunit by library screening

A cDNA library of rat total brain in λgt11 (Clontech, Palo Alto, CA) was screened by plaque hybridization method to isolate the full-length cDNA of the BK_{Ca} channel β4-subunit (rβ4). The entire open reading-frame (ORF) region of human β4 cDNA (*KCNMB4* or hβ4) was used as a hybridization probe for initial screening. The hβ4 cDNA was amplified by polymerase chain reaction (PCR), gel purified, and then labeled with ^{32}P using random-primer extension (Amersham Pharmacia, Piscataway, NJ). Positive clones of the first-round screening were further purified up to four consecutive rounds. The DNA inserts were isolated and subcloned into a plasmid, pBluescript II (Stratagene, La Jolla, CA). DNA sequences of the inserts were determined more than three times in both directions using an automatic DNA sequencer (Perkin-Elmer, Shelton, CT).

Functional expression of rβ4 and rat BK_{Ca} channel α-subunit in *Xenopus* oocytes

The rβ4 and the rat BK_{Ca} channel α-subunit (rSlo) cDNAs were subcloned into pGH vector for expression in *Xenopus* oocytes. The sequence information of rSlo used in this study can be obtained from GenBank accession number AF135265 (Ha et al., 2000). This rSlo clone is expressed highly in rat brain and contains the insertions of 4, 0, 0, and 27 amino acid residues at splicing sites 1–4, respectively, when compared with that of human Slo (GenBank accession number U11717) (Tseng-Crank et al., 1994). The pGH expression vector contains the 5′- and 3′-untranslated regions of *Xenopus* β-globin gene and is known to enhance the protein expression of certain mammalian messages in *Xenopus* oocytes (Liman et al., 1992). Complementary RNA of each construct was prepared in vitro as described in previous studies (Ha et al., 2000; Soh and Park, 2001). Plasmid DNA was purified (Qiagen midi-prep columns, Qiagen, Valencia, CA) and digested with a restriction enzyme, *Not*I. Complementary RNA (cRNA) was synthesized from linearized plasmid DNA using T7 RNA polymerase in the presence of a cap analog, m7G(5′)ppp(5′)G, and nucleotide triphosphates. Oocytes of stages V and VI were surgically removed from the ovarian lobes of anesthetized female *Xenopus laevis* (*Xenopus*One, Dexter, MI) and transferred into Ca^{2+}-free OR medium (86 mM NaCl, 1.5 mM KCl, 2 mM $MgCl_2$, 10 mM HEPES, 50 μg/ml gentamycin (pH 7.6)). The follicular cell layer was removed by incubating oocytes in Ca^{2+}-free OR medium containing 3 mg/ml collagenases (Worthington Biochemical, Lakewood, NJ) for 2 h. The oocytes were then washed extensively with and kept in ND-96 medium (96 mM NaCl, 2 mM KCl, 1.8 mM $CaCl_2$, 1 mM $MgCl_2$, 5 mM HEPES, 50 μg/ml gentamicin (pH 7.6)) at 18°C. Each oocyte was injected with 50 nl of cRNA containing ~1 ng for single-channel recordings and 50 ng for macroscopic current recordings using a Drummond microdispenser (Broomall, PA), respectively. Injected oocytes were incubated at 18°C for 3–5 days in sterile ND-96 medium. Immediately before patch-clamp experiments, the vitelline membrane was removed with fine forceps.

Electrophysiological recordings and data analysis

All single-channel and macroscopic current recordings were performed using the giga-ohm seal patch-clamp method in either excised inside-out or outside-out configuration. Patch pipettes were fabricated from borosilicate glass (WPI, Sarasota, FL) and fire polished to the resistance of 2–5 MΩ for macroscopic patches and 5–8 MΩ for single-channel recording. For single-channel recordings, patch pipettes were coated with beeswax. The channel currents were amplified using an Axopatch 200B amplifier (Axon Instruments, Foster City, CA), low-pass filtered at 1 or 2 kHz using a four-pole Bessel filter, and digitized at a rate of 10 or 20 points/ms using Digidata 1200A (Axon Instruments). No series resistance compensation was used and linear leak currents were subtracted from macroscopic currents.

For single-channel recordings, membrane patches of inside-out configuration were held at various membrane potentials. Single rSlo or rSlo/rβ4 channels were readily activated at high levels of intracellular Ca^{2+}. For single-channel analysis, transitions between closed and open states were determined by setting the threshold at half of the unitary current amplitude. To determine the single-channel conductance of rSlo and rSlo/rβ4 channels, mean amplitudes of channel currents were obtained from histograms fit with Gaussian distributions and the mean current levels were plotted against transmembrane voltages. Slope conductance value was obtained by linear regression. Dwell times of open and closed events recorded for single rSlo and rSlo/rβ4 channels were analyzed using the logarithmic binning method. The dwell-time distributions were fitted with two exponentials using simplex-least-squares fitting methods (Fechan and pSTAT, Axon Instruments). The peaks in the dwell-time distributions fall at the time constants of each exponential component.

Macroscopic currents of the BK_{Ca} channel were activated by voltage pulses delivered from a holding potential of -100 mV to membrane potentials ranging from -140 to 140 mV in 10-mV or 20-mV increments. Recording solutions for both single and macroscopic channels expressed in oocytes contained gluconates as a nonpermeant anion to prevent the activation of endogenous calcium-activated chloride channels. The intracellular and extracellular solutions contained the following components unless specified otherwise (in mM): 120 potassium gluconate, 10 HEPES, 4 KCl, and 5 EGTA (pH 7.2). $CaCl_2$ was added into intracellular solution to provide the required free-Ca^{2+} concentration (0.1–20 μM) calculated using a stability constant for Ca-EGTA of 10.86, and the calculation included a pH adjustment (Martell and Smith, 1974). To compare the characteristics of the channels accurately, an identical set of intracellular solutions was used throughout the entire experiments: single and macroscopic current recordings, and the recordings of the channels composed of both rSlo alone and rSlo with rβ4. Commercial software packages such as Clampex 8.0 or 8.1 (Axon Instruments), and Origin 6.1 (OriginLab, Northampton, MA) were

used for the acquisition and the analysis of single-channel and macroscopic recording data.

Statistical analysis

All data were presented as means ± SE and n indicates the number of independent experiments. For each data set, the statistical significance of the difference was tested using ANOVA for independent observations. In all cases $P < 0.01$ was considered significant. Each macroscopic current trace represents an average of three records in succession.

RESULTS

Isolation of cDNA for β4-subunit of rat BK_{Ca} channel and its molecular biological characterization

To obtain the cDNA of the BK_{Ca} channel β4-subunit expressed in rat brain, we screened 2.7×10^6 plaque-forming unit of rat total brain cDNA library and isolated a single clone covering the full length of the β4 open reading frame. The full-length cDNA, named as rβ4, was 1,028 bp with a 633-bp-long ORF and encodes a protein product of 210 amino acids (GenBank accession number AY028605). When compared with other family members of human BK_{Ca} channel β-subunits, the deduced amino acid sequences of rβ4 showed ~18%, 25%, 22%, and 94% to hβ1, hβ2, hβ3, and hβ4, respectively. The open reading frame and deduced amino acid sequence of rβ4 were compared to the previous reported orthologs of human β4 (hβ4, GenBank accession number AF207992) and mouse β4 (mβ4, GenBank accession number AF215892). The rβ4 were ~94% and 99% identical to hβ4 and mβ4, respectively. The amino acid sequence of rβ4 and mβ4 was identical except only a single residue at position 169 (valine for rβ4 and alanine for mβ4). The hydrophobicity analysis of the rβ4-subunit using Kyte-Dolittle methods predicted two putative transmembrane regions and a large extracellular loop amino acid sequence (data not shown) as adopted in the previous study with mβ4.

To check whether any alternative splicing variants of rβ4 occur in different regions of rat brain, we prepared total RNAs from five distinct regions of rat brain (whole brain, cerebral cortex, mid brain, cerebellum, and brain stem) and performed reverse transcriptase-polymerase chain reaction (RT-PCR). We initially noticed that the open reading frame of the human β4 gene is encoded by three different exons separated by ~27- and 33-k basepairs in human chromosome 12q14.1–15. A pair of DNA primers was designed to recognize the entire open reading frame of rβ4 coding regions. The RT-PCR resulted in single amplified DNA bands with an identical size in all five different subregions of the brain. The sequencing analysis of RT-PCR products also confirmed that only a single type of rβ4 message identical to the clone we obtained was expressed in different regions of rat brain (data not shown).

Effects of rβ4 on conductance-voltage relationship of rSlo channel

To investigate the detailed functional effects of rβ4 on rSlo channels, cRNAs of rSlo and rβ4 were synthesized in vitro and injected into *Xenopus* oocytes. We usually used 12-fold molar excess of the rβ4 transcripts to ensure the sufficient coassembly of the rβ4-subunit with the rSlo subunit. From 3 to 5 days after injection, macroscopic channel activities of rSlo and rSlo coexpressed with rβ4 were measurable. Representative current traces from inside-out patch recordings are shown for rSlo (Fig. 1 *A*) and rSlo/rβ4 channels (Fig. 1 *B*). Recording in low and high free calcium required different voltage steps for rSlo and rSlo/rβ4 channels to reach the levels of steady-state activation. To obtain accurate maximum conductance and to compare distinct current characteristics between rSlo and rSlo/rβ4, macroscopic rSlo and rSlo/rβ4 channel currents were elicited with 50-ms, 100-ms, or 200-ms-long voltage steps in different intracellular calcium concentrations. The representative traces were obtained using voltage steps of 100 ms and 200 ms for rSlo and rSlo/rβ4 channels, respectively. The activation of channel currents at various test potentials was measured using tail currents at 0.8 or 1 ms after repolarization to −100 mV. The activation of macroscopic currents of both rSlo and rSlo/rβ4 channels was highly dependent on intracellular Ca^{2+} concentrations and membrane potentials.

Based on the current recordings such as those shown in Fig. 1, *A* and *B*, we plotted the conductance-voltage (*G-V*) relationship and determined the half-activation voltages ($V_{1/2}$) of both rSlo and rSlo/rβ4 at various intracellular Ca^{2+} concentrations (Fig. 1, *C–E*). At submicromolar free Ca^{2+}, the coexpression of rβ4 shifted *G-V* curves of the rSlo channel slightly but significantly to the right (e.g., 0.5 μM; *open* and *solid circles* in Fig. 1, *C* and *D*). However, the *G-V* curves were shifted toward the left direction at higher intracellular free Ca^{2+} concentrations >1 μM. The $V_{1/2}$ values of rSlo and rSlo/rβ4 channels were plotted against intracellular concentrations of Ca^{2+}, $[Ca^{2+}]_i$ (Fig. 1 *E*). When the intracellular Ca^{2+} is increased from 0.5 μM to 20 μM, the membrane voltage required for half-activation of rSlo channel is decreased from 146 ± 7 mV to −22 ± 3 mV. The same changes in Ca^{2+} concentration decreased $V_{1/2}$ of rSlo/rβ4 from 155 ± 4 mV to −58 ± 2 mV. Although the rβ4-subunit shifted $V_{1/2}$ of rSlo to the positive voltage ranges at 0.5 μM $[Ca^{2+}]_i$, the direction of shift was changed toward negative in the presence of $[Ca^{2+}]_i$ >1 μM. At 20 μM $[Ca^{2+}]_i$, the β4-subunit shifted the $V_{1/2}$ of rSlo ~37 mV toward negative voltages.

In a series of previous studies, a modified version of the Monod-Wyman-Changeux (MWC) model for allosteric proteins was applied successfully to explain gating properties of BK_{Ca} channels (Cui et al., 1997; Cox et al., 1997, Cox and Aldrich, 2000). Based on the ''two-tiered gating scheme,'' Cox and Aldrich applied a voltage-dependent

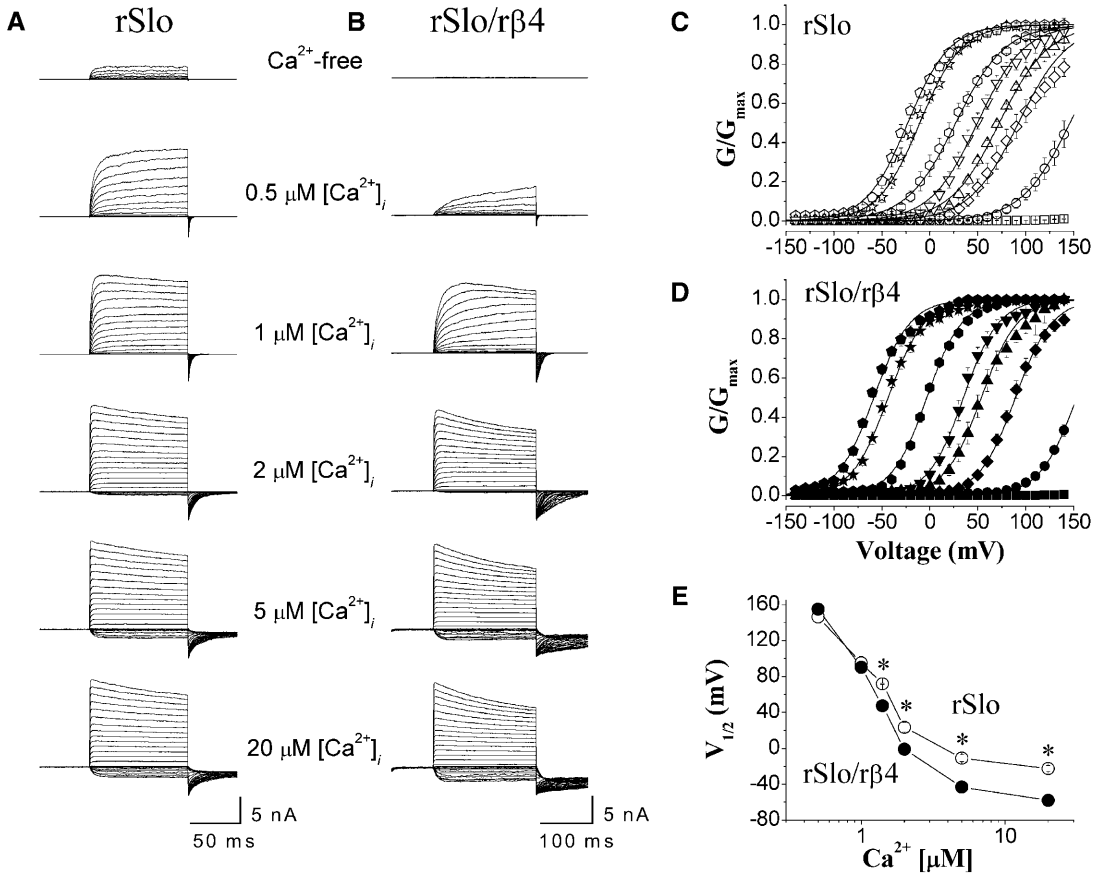

FIGURE 1 Representative current traces from excised patches expressing rSlo and rSlo/rβ4 channels and effects of rβ4-subunit on the conductance-voltage relationship of rSlo channels. Macroscopic currents of rSlo (*A*) and rSlo/rβ4 (*B*) were recorded in symmetrical 124 mM K^+-gluconate. The concentrations of intracellular free Ca^{2+}, $[Ca^{2+}]_i$, were indicated. Ionic currents were elicited with voltage steps of 100 ms for rSlo and 200 ms for rSlo/rβ4 to test potentials ranging from -140 mV to 140 mV in 10-mV increments. The holding voltage was -100 mV. Each current trace represents an average of three records in succession. Tail currents of each test potential were determined at 0.8 or 1 ms after repolarization to -100 mV. The conductance-voltage (*G-V*) relationship for rSlo (*C*) and rSlo/rβ4 (*D*) were shown. The concentrations of intracellular free calcium were shown as follows: Ca^{2+}-free (*squares*), 0.5 μM (*circles*), 1 μM (*diamonds*), 1.4 μM (*up triangles*), 1.7 μM (*down triangles*), 2 μM (*hexagons*), 5 μM (*asterisks*), and 20 μM (*pentagons*). The solid lines represent the best fit of the VD-MWC model, $P_{open} = 1/[1 + \{(1 + [Ca^{2+}]/K_C)/(1 + [Ca^{2+}]/K_O)\}^4 L(0) e^{-QFV/RT}]$, proposed previously for mSlo channel (Cox and Aldrich, 2000). $L(0)$ represents the open-to-closed equilibrium constant in the absence of an applied voltage, Q the equivalent gating charge associated with this equilibrium, K_C the closed-conformation Ca^{2+} dissociation constant, and K_O the open-conformation Ca^{2+} dissociation constant. Parameters of the fits are as follows: for rSlo, $L(0) = 942.86 \pm 36.89$, $Q = 1.04 \pm 0.04$, $K_O = 0.62 \pm 0.06$ μM, $K_C = 6.57 \pm 0.48$ μM; for rSlo/rβ4, $L(0) = 980$, $Q = 1.35$, $K_O = 1.2$ μM, $K_C = 0.6$ μM at 0.5 μM $[Ca^{2+}]$; $L(0) = 980$, $Q = 1.35$, $K_O = 0.66$ μM, $K_C = 6.2$ μM at 1 μM, 1.4 μM, and 1.7 μM $[Ca^{2+}]$; $L(0) = 600$, $Q = 1.37$, $K_O = 0.42$ μM, $K_C = 8.43$ μM at 2 μM, 5 μM, and 20 μM $[Ca^{2+}]$. (*E*) Relationship between intracellular Ca^{2+} concentration and the half-activation voltages. Each data point was obtained from the best fits of Boltzmann function, $G/G_{max} = 1/[1 + \exp\{zF(V_{1/2} - V)/RT\}]$, from independent data sets. Data points for rSlo and rSlo/rβ4 are denoted as open and solid symbols, respectively. Each data point represents the mean $\pm$ SE from at least 10 recordings of six different oocytes. Asterisks represent the significant differences tested using ANOVA test for independent observations ($P < 0.01$).

version of the MWC (VD-MWC) model to interpret the activation of mouse Slo (mSlo) (Cox and Aldrich, 2000). Although the model was simple and includes several assumptions, many aspects of the mSlo channel especially the effects of Ca^{2+} and voltage could be interpreted successfully. We applied the VD-MWC model to our experimental results and simulated the effects of rβ4. The solid lines in Fig. 1, *C* and *D*, represent the best fit of a VD-MWC model coplotted with experimental data. The rβ4-subunit increased the apparent affinity of the rSlo channel for Ca^{2+} >2 μM (the dissociation constant for Ca^{2+} in closed conformation, K_C: 6.57 $\pm$ 0.48 for rSlo, 8.4 $\pm$ 0.97 for rSlo/rβ4; the dissociation constant for Ca^{2+} in open conformation, K_O: 0.62 $\pm$ 0.06 for rSlo, 0.42 $\pm$ 0.03 for rSlo/rβ4). However, the apparent Ca^{2+} affinity of rSlo/rβ4 was decreased dramatically at lower Ca^{2+} concentrations (K_C: 6.57 for rSlo, 0.6 for rSlo/rβ4; K_O: 0.62 for rSlo, 1.2 for rSlo/rβ4). At intermediate Ca^{2+} concentrations (e.g., 1.4 μM and 1.7 μM Ca^{2+}), the rβ4-subunit did not affect the Ca^{2+} affinity significantly (K_C: 6.57 for rSlo, 6.2 for rSlo/rβ4; K_C: 0.62 for rSlo, 0.66 for rSlo/rβ4).

In summary, the β4-subunit increased the voltage range of the BK_{Ca} channel activation in a Ca^{2+}-dependent manner. This effect of the β4-subunit should be more prominent when

the intracellular Ca^{2+} concentrations are relatively high. Although the rSlo channels evoke only 12% of maximal currents at −50 mV in the presence of 5 μM, the rSlo/rβ4 channel can be activated to 45% under the identical conditions.

Effects of β4-subunit on activation and deactivation kinetics of macroscopic rSlo channel currents

As shown in the raw traces of Fig. 1, *A* and *B*, the gating kinetics of macroscopic rSlo channel currents was significantly affected by the coexpression of the rβ4-subunit. The ionic currents of the initial 100 ms and 200 ms activated by a step pulse from −140 mV to 140 mV were measured for the rSlo and rSlo/rβ4 channels, respectively, at different $[Ca^{2+}]_i$, and normalized to the maximum current levels for direct comparison (Fig. 2 *A*). The coexpression of rβ4 decreased the activation rate of the rSlo channels at low intracellular Ca^{2+} such as at 0.5–1 μM (Fig. 2 *A*, *left* and *middle panels*). However, this effect of rβ4 disappeared gradually as the concentration of intracellular Ca^{2+} was increased and the activation of rSlo became faster (Fig. 2 *A*, *right panel*). The activation time constants of the rSlo and rSlo/rβ4 channel currents were estimated by fitting the current traces to single exponentials and the activation rates ($1/\tau$) were plotted as a function of membrane potentials in Fig. 2 *B*. Not only the activation rates but also the voltage dependence of the rSlo channel activation were significantly altered. The activation rates of the rSlo/rβ4 channel were less sensitive to the transmembrane voltages compared with those of rSlo at identical $[Ca^{2+}]_i$ and the trend was more dramatic as the concentration of Ca^{2+} was decreased. In fact, the activation of rSlo/rβ4 was almost insensitive to transmembrane voltage at 0.5 μM and 1 μM of $[Ca^{2+}]_i$ (Fig. 2 *B*, *solid circles* and *triangles* in *right panel*).

The deactivation rates of rSlo were also decreased by the coexpression of the rβ4-subunit. In Fig. 2 *C*, the rSlo and rSlo/rβ4 channels were preactivated to 100 mV and then the deactivation of the channel currents were observed at −80 mV. The slowing of deactivation was evident in the normalized current traces at all three different $[Ca^{2+}]_i$ tested, although the effects were most dramatic at 2 μM of $[Ca^{2+}]_i$ (Fig. 2 *C*, *right panel*). The deactivation time constants of the rSlo and rSlo/rβ4 channel currents were estimated by fitting the current traces to single exponentials and the deactivation rates ($1/\tau$) were plotted in Fig. 2 *D*. The deactivation rates of rSlo coexpressed with rβ4 were lower than those of rSlo at all membrane potentials and intracellular Ca^{2+} concentrations tested. Therefore, the β4-subunit decreases both the activation and the deactivation rates of macroscopic rSlo currents. Although rSlo/rβ4 channels tend to respond to the changes in transmembrane voltage more slowly, the exact effects of rβ4 on the gating kinetics of rSlo are complex and influenced by transmembrane voltages as well as intracellular concentrations of Ca^{2+}.

Effects of β4-subunit on Ca^{2+}-dependent activation of single rSlo channels

To reveal the detailed functional effects of the rβ4-subunit, rSlo and rSlo/rβ4 channels were investigated at the single-channel level. To confirm the excised inside-out patches containing a single channel, we recorded the channel currents in extended periods at high levels of intracellular Ca^{2+} or depolarized potentials expected to activate readily the expressed channels. Single-channel recordings were performed in various durations for investigation of steady-state kinetics. We recorded for 3–5 min (up to 2000 of the channel transitions) at low Ca^{2+} concentrations and for 0.5–2 min (up to 10,000 of the channel transitions) at high levels of Ca^{2+}. Representative traces of single rSlo (Fig. 3 *A*) and rSlo/rβ4 channels (Fig. 3 *B*) were shown. The currents were recorded at 40 mV under various $[Ca^{2+}]_i$. The openings of single rSlo and rSlo/rβ4 channels were highly dependent on the intracellular Ca^{2+} concentrations as expected. Although the single-channel conductance of rSlo was not altered by the coexpression of rβ4 (data not shown), the gating behavior of single rSlo/rβ4 channels was significantly different from those of rSlo channels. The individual open events of the rSlo/rβ4 channel recorded at low $[Ca^{2+}]_i$ was much longer compared with those of rSlo channels (see 1-μM *traces* in Fig. 3 shown in two different timescales). Especially, single-channel transitions of rSlo/rβ4 channels were remarkably slower than rSlo channels at low Ca^{2+} such as 0.5 μM and 1 μM Ca^{2+}.

In Fig. 4, we compared the activation of rSlo and rSlo/rβ4 by intracellular Ca^{2+} measured at single-channel and macroscopic current levels. The activation of macroscopic currents (G/G_{max}) and the open probability of single channels (P_o) were coplotted against intracellular concentration of Ca^{2+} for rSlo (Fig. 4 *A*, *open diamonds* for G/G_{max} and *open squares* for P_o) and rSlo/rβ4 (Fig. 4 *B*, *open triangles* for G/G_{max} and *open circles* for P_o), respectively. For both rSlo and rSlo/rβ4 channels, the macroscopic activation curves were superimposed well with the open probability of single channels, indicating that the increase in macroscopic currents of each channel by intracellular Ca^{2+} were entirely due to the increase in the open probability of the channel. The effects of the rβ4-subunit on the cooperative opening of rSlo by intracellular Ca^{2+} were shown in Fig. 4 *C*, where the open probability of single rSlo (*open squares*) and rSlo/rβ4 channels (*open circles*) were compared. The increase in open probability of the rSlo channel by Ca^{2+} became much more sensitive by the coexpression of rβ4. Although the Ca^{2+} dependence of rSlo was best fitted with the Hill coefficient of 3.2 ± 0.3, that of rSlo/rβ4 was estimated as 6.5 ± 0.2. Due to the highly cooperative activation by intracellular Ca^{2+}, the open probabilities of single rSlo/rβ4 channels were significantly lower than those of rSlo channels under micromolar Ca^{2+} concentrations (Fig. 4 *D*). At 0.5 μM Ca^{2+}, the open probability was 0.025 ± 0.009 for rSlo and 0.008 ± 0.001

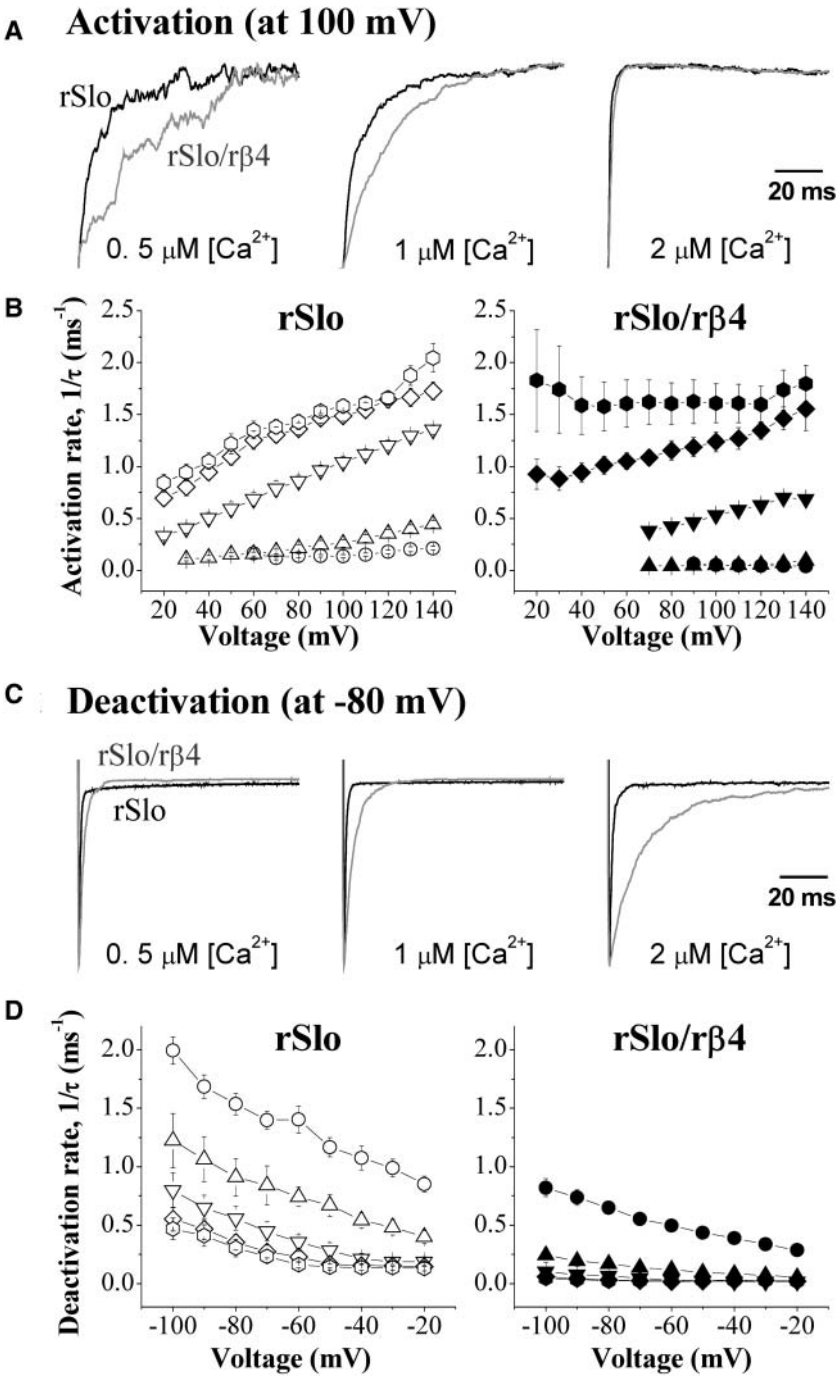

FIGURE 2 Activation and deactivation kinetics of rSlo and rSlo/rβ4 channels. (*A*) Activation characteristics of rSlo and rSlo/rβ4 channels. Channel currents of rSlo (*black*) and rSlo/rβ4 (*gray*) activated by a step pulse from −100 mV to 100 mV were normalized with their maximum currents. (*C*) Deactivation characteristics of rSlo and rSlo/β4 channels. Tail currents were elicited with 100-ms voltage steps to test potentials ranging from −100 mV to 20 mV in 20-mV increments from a prepulse at 100 mV. Tail currents were normalized with their maximum currents. Activation and deactivation rate ($1/\tau$) of macroscopic rSlo (*B*) and rSlo/rβ4 (*D*) were plotted as a function of membrane voltage. Activation and deactivation time constant (τ) of macroscopic rSlo and rSlo/rβ4 channel currents were obtained by fitting the individual current traces to simplex single exponential function. The concentrations of intracellular free calcium were as follows: 0.5 μM (*circles*), 1 μM (*up triangles*), 2 μM (*down triangles*), 5 μM (*diamonds*), and 20 μM (*hexagons*). Data points for rSlo and rSlo/rβ4 are denoted as open and solid symbols, respectively. Each data point represents the mean ± SE from at least eight independent recordings.

for rSlo/rβ4. As the Ca^{2+} concentration was increased beyond 1.4 μM, the open probabilities of rSlo/rβ4 were dramatically increased and much higher than those of rSlo channels. The results were consistent with the findings that the $V_{1/2}$ values of macroscopic rSlo/rβ4 became significantly more negative than those of rSlo only at >1.4 μM Ca^{2+} (Fig. 1, *C–E*). It was also worth noticing that the $V_{1/2}$ of rSlo/rβ4 in the same figure was estimated even slightly more positive than that of rSlo at 0.5 μM Ca^{2+}.

Effects of β4-subunit on steady-state gating of single rSlo channels

As shown in Fig. 3, the opening and closing of single rSlo/rβ4 channels were much slower than those rSlo qualitatively. We further investigated and quantified the effects of the rβ4-subunit on the single-channel kinetics of the rSlo channel. In Fig. 5, the representative dwell-time histograms of open and closed events were shown for rSlo and rSlo/rβ4 channels at

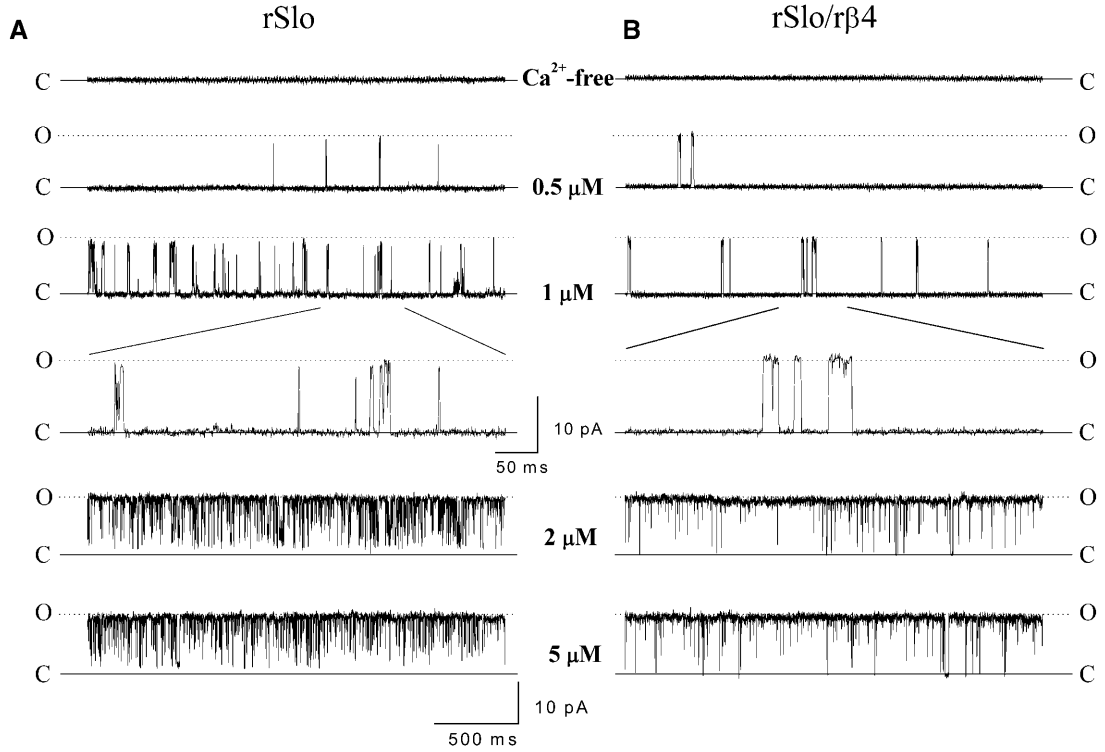

FIGURE 3 Representative single-channel currents of rSlo and rSlo/rβ4 expressed in *Xenopus* oocytes. Typical single-channel current recordings of rSlo (*A*) and rSlo/rβ4 (*B*) channels were shown at different intracellular Ca^{2+} concentrations. Ionic currents of single channels in a patch of oocytes membrane were continuously recorded at 40 mV in different intracellular Ca^{2+} concentrations. Activity of the single channel was highly dependent on the concentration of intracellular Ca^{2+}. The data were sampled at 10 kHz or 20 kHz and filtered at 2 kHz. Single-channel currents of rSlo and rSlo/rβ4 were measured under identical recording solutions for macroscopic channel currents recording as previously shown in Fig. 1.

0.5 μM (*A*), 1 μM (*B*), and 2 μM (*C*), respectively. We reported previously that both open and close dwell times of the rSlo channel were well fitted with a combination of two exponential components of fast and slow (Ha et al., 2000). We also used two exponentials to fit both open and closed events of single rSlo/rβ4 channels and determined the mean dwell times of open and closed events. It was readily noticeable that rSlo/rβ4 channels exhibited the different dwell-time distributions as well as the altered ratios between fast and slow components for both open and closed events. Thus, the steady-state gating kinetics and kinetic components were significantly affected by coexpression of β4.

In Fig. 6, the mean dwell times of both open and closed events were compared in different concentrations of intracellular Ca^{2+}. The effect of rβ4 on single rSlo channels was multiple and also dependent on the concentration of intracellular Ca^{2+}. The coexpression of rβ4 increased the mean dwell times of open events and thus decreased the closing rates of the rSlo channel. Although the effects of the rβ4-subunit were somewhat sensitive to $[Ca^{2+}]_i$, 5- to 10-fold increases in the open time constant were observed for the slower component of open events (Fig. 6 *A*, *top panel*). The rβ4-subunit also increased the open time constant of the fast component significantly but no more than twofold. In the case of the closed time constants, the significant effects of the rβ4-subunit were only detected for the slower component and the effects were highly sensitive for $[Ca^{2+}]_i$ (Fig. 6 *B*, *top panel*). Although about fivefold increase in the closed time constant was seen at 0.5 and 1 μM, the effects were minimal at >2 μM $[Ca^{2+}]$. Therefore, rSlo/rβ4 channels have longer dwell times for both open and closed states at the single-channel level in general and thus the coexpression of the rβ4-subunit tends to slow down the steady-state gating transitions of rSlo channels.

DISCUSSION

In this study, we isolated a full-length cDNA encoding the β4-subunit of the BK_{Ca} channel from the rat brain and revealed its functional effects on the pore-forming rat α-subunit, rSlo, using electrophysiological means. The amino acid sequence of rat β4 shows that the protein is highly conserved among different mammalian species (Brenner et al., 2000; Behrens et al., 2000; Weiger et al., 2000). Although the membrane topology of different β-subunits was predicted to be similar, the sequence identity among β1–β4-subunits was relatively low and the expression of the β4-subunit message was expressed concentrated in the central nervous system as previously reported for human and mouse. Unlike the α-subunit of BK_{Ca} channel known to

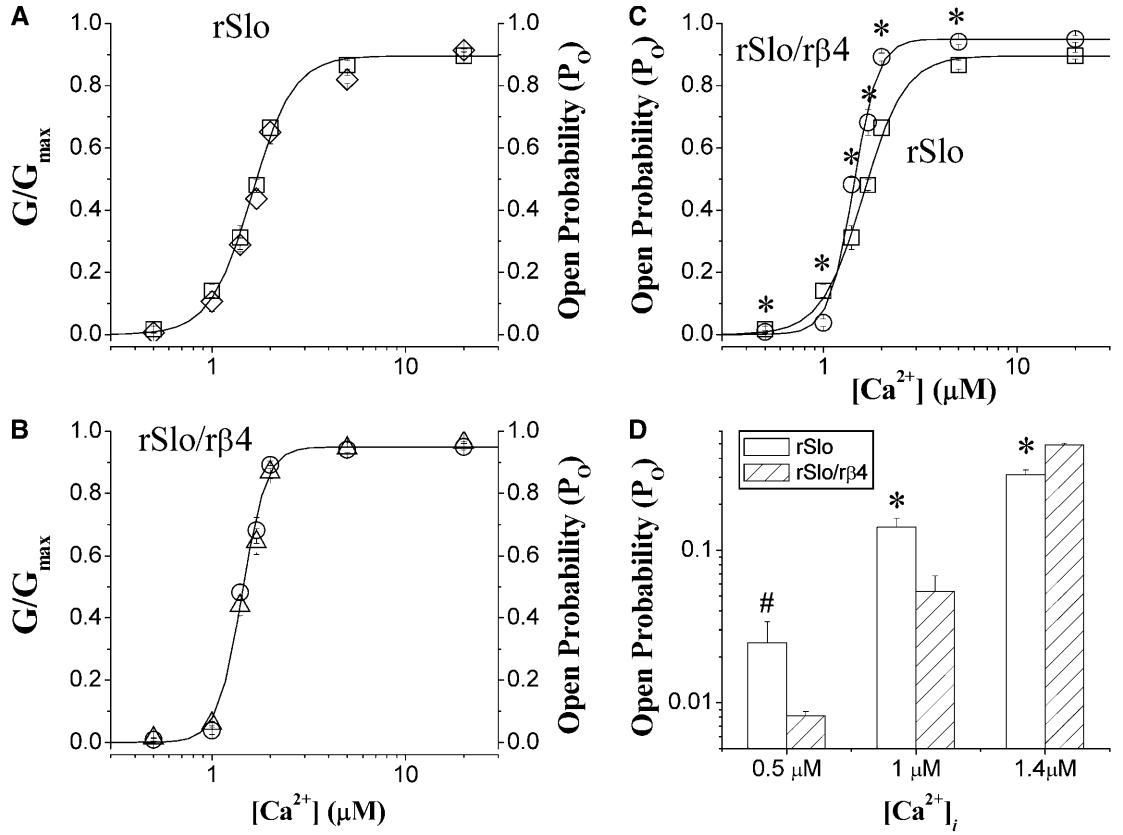

FIGURE 4 Comparison between open probability for single channels and activation of macroscopic currents for rSlo and rSlo/rβ4 channels by Ca^{2+}. Single-channel open probability of rSlo (*A*, □) and rSlo/rβ4 (*B*, ○) recorded with various intracellular Ca^{2+} concentrations were coplotted with the activation of macroscopic channel currents (rSlo, ◇; rSlo/rβ4, Δ). Recording of both single and macroscopic currents were obtained at 40 mV. (*C*) Relationship of open probability against intracellular Ca^{2+} concentration of rSlo (□) and rSlo/rβ4 (○) was fitted to the Hill equation. (*D*) Open probability single rSlo (*open bars*) and rSlo/rβ4 (*striped bars*) determined at 0.5, 1, and 1.4 μM of intracellular Ca^{2+}. The mean values of the open probability for each channel was given in the text. Identical recording solutions were used for both macroscopic and single-channel recordings. Each data point represents the mean ± SE from eight (for rSlo) and nine (for rSlo/rβ4) independent recordings. Asterisks represent the significant differences tested using ANOVA test for independent observations, (#, $P < 0.05$; *, $P < 0.01$).

produce multiple splicing variants of functional significance, we failed to detect any splicing variant in the coding region of the β4-subunit from subregions of rat brain. Thus, we suggest that the rβ4 clone used in this study is expressed dominantly, if not exclusively, in rat brain and coassembles with the diverse splicing variants of the α-subunit to form functional BK_{Ca} channels. However, this as well as the previous studies do not rule out the possibility that some BK_{Ca} channels in brain neurons may exist as homotetramer of α-subunits without the coassembly of the β4-subunit.

Compared with the rSlo channel (or BK_{Ca} channels of homotetrameric α-subunits) currents, the macroscopic currents of the rSlo/rβ4 channel showed the marked differences in the conductance-voltage relationship, the gating kinetics, and the cooperativity for intracellular Ca^{2+}. The activation of rSlo/rβ4 channels was affected differently depending on the concentration of intracellular calcium. Although the conductance-voltage curves were shifted only slightly to more depolarizing voltages at low Ca^{2+} concentration, the *G-V* relationship shifted dramatically more negative potentials at high Ca^{2+} concentration. As the results, the BK_{Ca} channels composed of rSlo and rβ4 can open at more hyperpolarized membrane voltages when the concentration of intracellular Ca^{2+} is progressively increased. Because the local concentration of intracellular Ca^{2+} is known to increase up to tens of micromolars during the action potential (Regehr and Tank, 1992), the half-activation voltages ($V_{1/2}$) are expected to shift >30 mV toward hyperpolarization direction. This result is also consistent with a previous report in which the effects of four different human β-subunits on *G-V* curves were compared (Brenner et al., 2000).

It was shown that the β1-subunit increased the apparent Ca^{2+} sensitivity by increasing open probability and shifted half-activation voltages to significantly more negative potentials (McManus et al., 1995; Knaus et al., 1994; Dworetzky et al., 1996; Cox and Aldrich, 2000; Nimigean and Magleby, 1999). Although the effect of rβ4 on conductance-voltage curves is similar to that of β1 at high

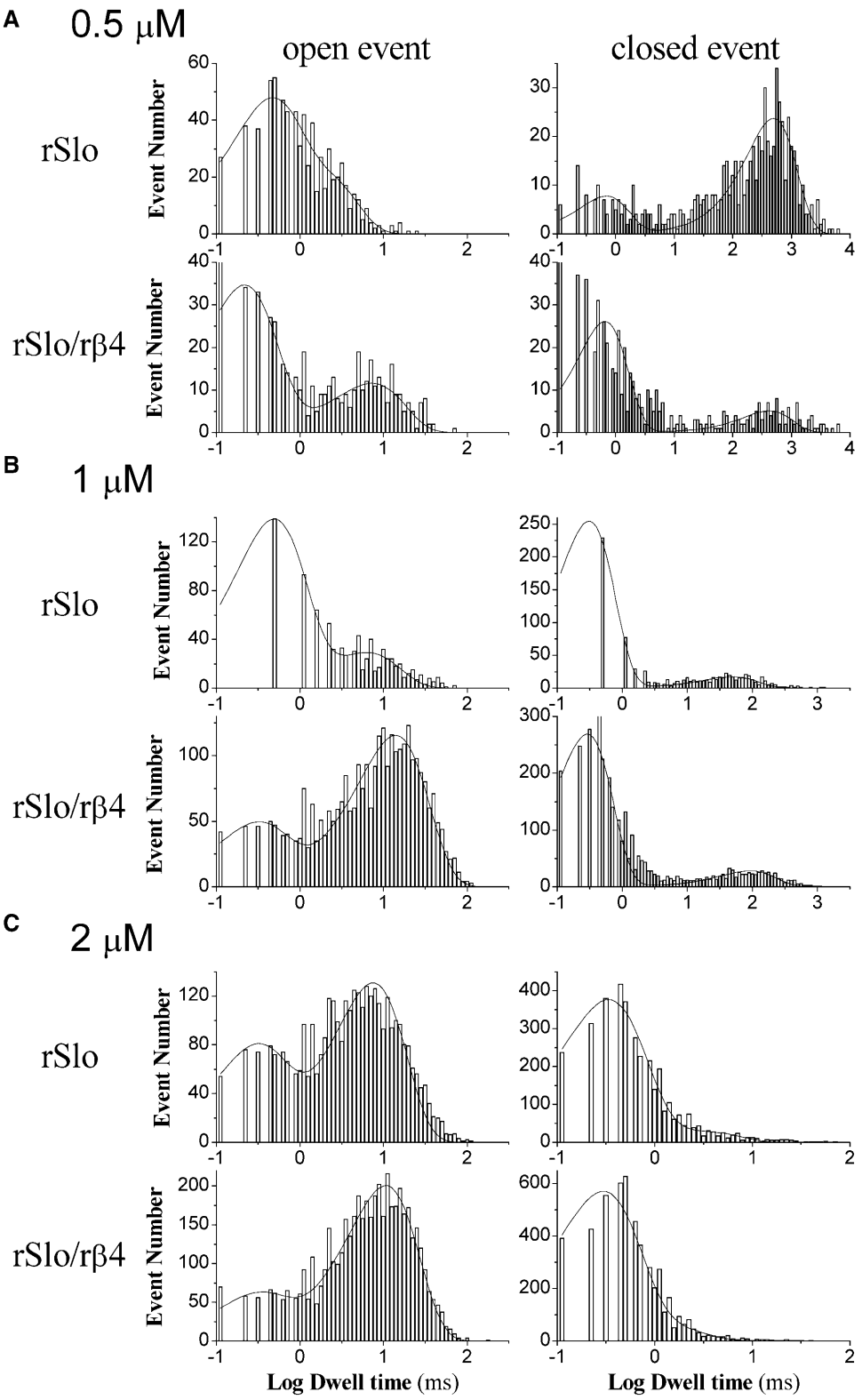

FIGURE 5 Representative dwell-time histograms of single rSlo and rSlo/rβ4 channels for open and closed events. Excised membranes were held at 40 mV in the presence of 0.5 μM (*A*), 1 μM (*B*), and 2 μM (*C*) intracellular Ca^{2+} concentrations. The histograms of both open and closed dwell times obtained from 2,000 (at low Ca^{2+} concentrations, continuously recorded for 3–5 min) to 10,000 (at high Ca^{2+} concentrations, continuously recorded for 0.5–2 min) transitions were plotted in log-bin timescales and fitted with a combination of two exponential functions. Solid lines on the bar graphs represent the sum of two exponential functions of time constants, τ_1 and τ_2.

Ca^{2+} concentrations, rβ4 slightly but significantly changes the voltage dependence of rSlo channel at low Ca^{2+} concentrations. The simulation of the VD-MWC model based on our experimental data provided valuable information on the effects of β4 on the gating of the rSlo channel. Although the rβ4-subunit increased the apparent affinity of the rSlo channel for Ca^{2+} >2 μM similar to the β1-subunit (Cox and Aldrich, 2000), the apparent affinity of

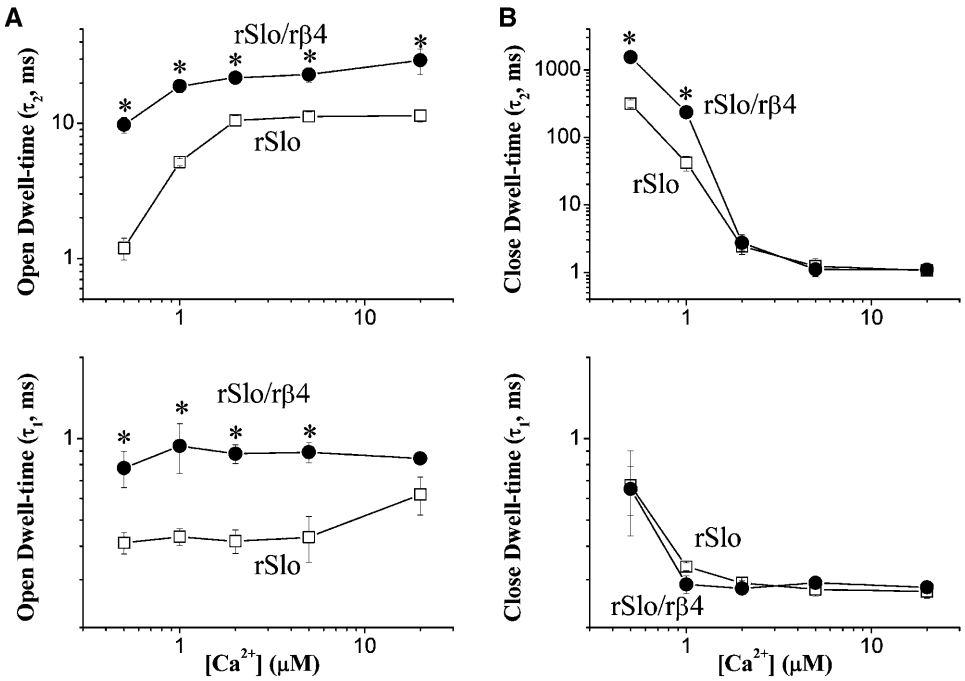

FIGURE 6 Effects of rβ4 on the steady-state gating kinetics of single rSlo channels. Time constants of open (*A*) and closed events (*B*) for rSlo (□) and rSlo/rβ4 (●) were plotted as a function of intracellular Ca^{2+} concentrations. The time constants, τ_1 and τ_2, represent the faster and slower components of open and closed dwell times. Each data point represents the mean ± SE from at least six independent single-channel recordings. Asterisks represent the significant differences tested using ANOVA for independent observations ($P < 0.01$).

rSlo/rβ4 for Ca^{2+} was decreased dramatically at lower Ca^{2+} concentrations. Therefore, the effects of the rβ4-subunit are quite different from those of the β1-subunit, because the β1-subunit increases the Ca^{2+} affinity regardless of its concentration. The β4-subunit increases the affinity for Ca^{2+} to the closed state of the Slo channel and thus makes the channel close at low Ca^{2+}. In high Ca^{2+}, however, the same subunit increases the affinity for Ca^{2+} to the open state and tends to open the channel. Thus, the β4-subunit makes the correlation between the changes in $V_{1/2}$ and $[Ca^{2+}]_i$ and broadens the effective ranges of voltage-dependent activation under various intracellular Ca^{2+} concentrations (Fig. 1 *E*). In general, the neuronal BK_{Ca} channels containing the β4-subunit would require significantly lower voltages to be activated at Ca^{2+} concentration >1 μM. Because the BK_{Ca} channels coassembled with β4 exhibits higher cooperativity for Ca^{2+} (Fig. 4), the channels should be able to respond more sensitively to the increase in intracellular Ca^{2+}. It is also intriguing that the same channels may not be activated efficiently under submicromolar concentrations of local Ca^{2+} under physiological transmembrane voltages (Fig. 4, *C* and *D*).

Functional rSlo channels are activated and deactivated rapidly in response to depolarizing and hyperpolarizing step pulses of membrane voltages. The kinetics of macroscopic currents becomes much slower when rSlo assembles with rβ4. The kinetics of rSlo/rβ4 channels was less dependent upon the membrane potential and significantly slower compared with those of rSlo. Thus, the slowing of macroscopic gating events may render significant physiological consequences. For an example, whereas the effects of the β4-subunit on the activation of BK_{Ca} channels is minimal at 10 μM, the deactivation of channel current is more than two-fold slower throughout the transmembrane voltage and thus the hyperpolarizing effects of the BK_{Ca} channel would be significantly longer. It remains to be determined how the gating effects of the β4-subunit are represented in the firing pattern of neuronal action potentials and the modulation of neuroexcitability. The β4-subunit also affects the steady-state gating behavior of BK_{Ca} channels. Although the rSlo channels showed rapid transitions between open and close states, much longer opening and closing events were observed for rSlo/rβ4. The most dramatic effect of the β4-subunit on the single BK_{Ca} channel was the decrease in closing and opening rates for the slow component at marginal concentration of Ca^{2+}.

One of the most noticeable effects of the β4-subunit revealed in this study was dramatic increase in the Ca^{2+} cooperativity for the BK_{Ca} channel. Although the Ca^{2+}-dependnent activation of the rSlo channel can be fit with the Hill coefficient of ~3.2, that of rSlo/rβ4 was best fit with 6.5. The highly cooperative activation in the presence of the β4-subunit makes the BK_{Ca} channel more sensitive to the concentration changes in intracellular Ca^{2+}. About twofold increase in intracellular Ca^{2+} from 1 to 2 μM can result in almost full activation of BK_{Ca} channels composed of rSlo/rβ4 and the effects can be solely explained with the increase in the open probability of single BK_{Ca} channels. Knowing the fact that the BK_{Ca} channel is likely composed of four α-subunits, it is intriguing to find that the Hill coefficient for Ca^{2+} can be as high as about seven. It will be important to determine in the subsequent studies what is the molecular mechanism of this high Ca^{2+} cooperativity rendered by the β4-subunit especially in the context of protein structure. In

conclusion, the neuronal-specific β-subunit of β4 modulates the functional characteristics of the BK_{Ca} channel α-subunits by altering not only the gating kinetics but also the sensitivity and the cooperativity for intracellular Ca^{2+}. It would be required in future works to confirm the effects of the β4-subunit on neuronal BK_{Ca} channels in vivo and to elucidate the functional roles of this auxiliary subunit on the excitability of neuronal cells in the brain in situ.

The authors thank Dr. Richard W. Aldrich at Stanford University for the cDNA of the human BK_{Ca} channel β4-subunit. We also thank the other members of the Laboratory of Molecular Neurobiology at K-JIST for their valuable comments and timely help throughout the work. The nucleotide sequence of rat BK_{Ca} channel β4-subunit reported in this article was deposited in the GenBank with accession number AY028605.

This research was supported by research grants from the Ministry of Science and Technology of Korea (Brain Neurobiology Research, M1-0108-00-005), the Korea Science and Engineering Foundation (R02-2000-00192), and the Korea Research Foundation (BK21) to C.-S. Park.

REFERENCES

Adelman, J. P., K. Z. Shen, M. P. Kavanaugh, R. A. Warren, Y. N. Wu, A. Lagrutta, C. T. Bond, and R. A. North. 1992. Calcium-activated potassium channels expressed from cloned complementary DNAs. *Neuron.* 9:209–216.

Atkinson, N. S., G. A. Robertson, and B. Ganetzky. 1991. A component of calcium-activated potassium channels encoded by the *Drosophila* slo locus. *Science.* 253:551–555.

Behrens, R., A. Nolting, F. Reimann, M. Schwarz, R. Waldschutz, and O. Pongs. 2000. hKCNMB3 and hKCNMB4, cloning and characterization of two members of the large-conductance calcium-activated potassium channel β subunit family. *FEBS Lett.* 474:99–106.

Bielefeldt, K., and M. B. Jackson. 1994. Phosphorylation and dephosphorylation modulate a Ca^{2+}-activated K^+ channel in rat peptidergic nerve terminals. *J. Physiol.* 475:241–254.

Brenner, R., T. J. Jegla, A. Wickenden, Y. Liu, and R. W. Aldrich. 2000. Cloning and functional characterization of novel large conductance calcium-activated potassium channel β subunits, hKCNMB3 and hKCNMB4. *J. Biol. Chem.* 275:6453–6461.

Butler, A., S. Tsunoda, D. P. McCobb, A. Wei, and L. Salkoff. 1993. mSlo, a complex mouse gene encoding ''maxi'' calcium-activated potassium channels. *Science.* 261:221–224.

Cox, D. H., and R. W. Aldrich. 2000. Role of the β1 subunit in large-conductance Ca^{2+}-activated K^+ channel gating energetics. Mechanisms of enhanced Ca^{2+} sensitivity. *J. Gen. Physiol.* 116:411–432.

Cox, D. H., J. Cui, and R. W. Aldrich. 1997. Allosteric gating of a large conductance Ca^{2+}-activated K^+ channel. *J. Gen. Physiol.* 110:257–281.

Cui, J., D. H. Cox, and R. W. Aldrich. 1997. Intrinsic voltage dependence and Ca^{2+} regulation of mslo large conductance Ca^{2+}-activated K^+ channels. *J. Gen. Physiol.* 109:647–673.

Dworetzky, S. I., C. G. Boissard, J. T. Lum-Ragan, M. C. McKay, D. J. Post-Munson, J. T. Trojnacki, C. P. Chang, and V. K. Gribkoff. 1996. Phenotypic alteration of a human BK (hSlo) channel by hSlo β-subunit coexpression: changes in blocker sensitivity, activation/relaxation and inactivation kinetics, and protein kinase A modulation. *J. Neurosci.* 16:4543–4550.

Ha, T. S., S. Y. Jeong, S. W. Cho, H. Jeon, G. S. Roh, W. S. Choi, and C. S. Park. 2000. Functional characteristics of two BK_{Ca} channel variants differentially expressed in rat brain tissues. *Eur. J. Biochem.* 267:910–918.

Jan, L. Y., and Y. N. Jan. 1997. Cloned potassium channels from eukaryotes and prokaryotes. *Annu. Rev. Neurosci.* 20:91–123.

Kaczorowski, G. J., H. G. Knaus, R. J. Leonard, O. B. McManus, and M. L. Garcia. 1996. High-conductance calcium-activated potassium channels; structure, pharmacology, and function. *J. Bioenerg. Biomembr.* 28:255–267.

Knaus, H. G., K. Folander, M. Garcia-Calvo, M. L. Garcia, G. J. Kaczorowski, M. Smith, and R. Swanson. 1994. Primary sequence and immunological characterization of β-subunit of high conductance Ca^{2+}-activated K^+ channel from smooth muscle. *J. Biol. Chem.* 269:17274–17278.

Liman, E. R., J. Tytgat, and P. Hess. 1992. Subunit stoichiometry of a mammalian K^+ channel determined by construction of multimeric cDNAs. *Neuron.* 9:861–871.

Martell, A. E., and R. M. Smith. 1974. Critical Stability Constants, Vol. 1. Plenum Publishing Corp., New York. 469.

McManus, O. B., L. M. Helms, L. Pallanck, B. Ganetzky, R. Swanson, and R. J. Leonard. 1995. Functional role of the β subunit of high conductance calcium-activated potassium channels. *Neuron.* 14:645–650.

Nimigean, C. M., and K. L. Magleby. 1999. The β subunit increases the Ca^{2+} sensitivity of large conductance Ca^{2+}-activated potassium channels by retaining the gating in the bursting states. *J. Gen. Physiol.* 113:425–440.

Qian, X., C. M. Nimigean, X. Niu, B. L. Moss, and K. L. Magleby. 2002. Slo1 tail domains, but not the Ca^{2+} bowl, are required for the β1 subunit to increase the apparent Ca^{2+} sensitivity of BK channels. *J. Gen. Physiol.* 120:829–843.

Regehr, W. G., and D. W. Tank. 1992. Calcium concentration dynamics produced by synaptic activation of CA1 hippocampal pyramidal cells. *J. Neurosci.* 12:4202–4223.

Robitaille, R., and M. P. Charlton. 1992. Presynaptic calcium signals and transmitter release are modulated by calcium-activated potassium channels. *J. Neurosci.* 12:297–305.

Robitaille, R., M. L. Garcia, G. J. Kaczorowski, and M. P. Charlton. 1993. Functional colocalization of calcium and calcium-gated potassium channels in control of transmitter release. *Neuron.* 11:645–655.

Rosenblatt, K. P., Z. P. Sun, S. Heller, and A. J. Hudspeth. 1997. Distribution of Ca^{2+}-activated K^+ channel isoforms along the tonotopic gradient of the chicken's cochlea. *Neuron.* 19:1061–1075.

Sah, P. 1996. Ca^{2+}-activated K^+ currents in neurones: types, physiological roles and modulation. *Trends Neurosci.* 19:150–154.

Shipston, M. J. 2001. Alternative splicing of potassium channels: a dynamic switch of cellular excitability. *Trends Cell Biol.* 11:353–358.

Soh, H., and C. S. Park. 2001. Inwardly rectifying current-voltage relationship of small-conductance Ca^{2+}-activated K^+ channels rendered by intracellular divalent cation blockade. *Biophys. J.* 80:2207–2215.

Tian, L., R. R. Duncan, M. S. Hammond, L. S. Coghill, H. Wen, R. Rusinova, A. G. Clark, I. B. Levitan, and M. J. Shipston. 2001. Alternative splicing switches potassium channel sensitivity to protein phosphorylation. *J. Biol. Chem.* 276:7717–7720.

Toro, L., M. Wallner, P. Meera, and Y. Tanaka. 1998. Maxi-K_{Ca}, a unique member of the voltage-gated K^+ channel superfamily. *News Physiol. Sci.* 13:112–117.

Tseng-Crank, J., C. D. Foster, J. D. Krause, R. Mertz, N. Godinot, T. J. DiChiara, and P. H. Reinhart. 1994. Cloning, expression, and distribution of functionally distinct Ca^{2+}-activated K^+ channel isoforms from human brain. *Neuron.* 13:1315–1330.

Uebele, V. N., A. Lagrutta, T. Wade, D. J. Figueroa, Y. Liu, E. McKenna, C. P. Austin, P. B. Bennett, and R. Swanson. 2000. Cloning and functional expression of two families of β-subunits of the large conductance calcium-activated K^+ channel. *J. Biol. Chem.* 275:23211–23218.

Valverde, M. A., P. Rojas, J. Amigo, D. Cosmelli, P. Orio, M. I. Bahamonde, G. E. Mann, C. Vergara, and R. Latorre. 1999. Acute activation of Maxi-K channels (hSlo) by estradiol binding to the β subunit. *Science.* 285:1929–1931.

Wallner, M., P. Meera, and L. Toro. 1999. Molecular basis of fast inactivation in voltage and Ca^{2+}-activated K^+ channels: a transmembrane β-subunit homolog. *Proc. Natl. Acad. Sci. USA*. 96:4137–4142.

Weiger, T. M., A. Hermann, and I. B. Levitan. 2002. Modulation of calcium-activated potassium channels. *J. Comp. Physiol. A. Neuroethol. Sens. Neural. Behav. Physiol*. 188:79–87.

Weiger, T. M., M. H. Holmqvist, I. B. Levitan, F. T. Clark, S. Sprague, W. J. Huang, P. Ge, C. Wang, D. Lawson, M. E. Jurman, M. A. Glucksmann, I. Silos Santiago, P. S. DiStefano, and R. Curtis. 2000. A novel nervous system β subunit that downregulates human large conductance calcium-dependent potassium channels. *J. Neurosci.* 20:3563–3570.

Xia, X. M., J. P. Ding, and C. J. Lingle. 1999. Molecular basis for the inactivation of Ca^{2+}- and voltage-dependent BK channels in adrenal chromaffin cells and rat insulinoma tumor cells. *J. Neurosci*. 19:5255–5264.

Xia, X. M., J. P. Ding, X. H. Zeng, K. L. Duan, and C. J. Lingle. 2000. Rectification and rapid activation at low Ca^{2+} of Ca^{2+}-activated, voltage-dependent BK currents: consequences of rapid inactivation by a novel β subunit. *J. Neurosci.* 20:4890–4903.